Tunable excitation of two-dimensional plasmon modes in InGaAs/InP HEMT devices for terahertz detection

Nima Nader Esfahani*[a,b,c], Xin Qiao[a], Robert E. Peale[a], Walter R. Buchwald[b,d], Joshua R. Hendrickson[c] and Justin W. Cleary[c]
[a]Department of Physics, University of Central Florida, Orlando FL, USA 32816
[b]Solid State Scientific Corporation, Nashua, NH 03060
[c]Air Force Research Laboratory, Sensors Directorate, Wright Patterson AFB OH 45433
[d]Department of Physics, University of Massachusetts, Boston MA, USA 02125

ABSTRACT

THz electromagnetic waves resonantly excite plasmons in the two dimensional electron gas (2DEG) of high electron mobility transistors (HEMTs) via grating-gate couplers. These excitations can induce measureable photoresponse. Biasing the grating gate tunes the photoresponse via control of 2DEG carrier density. Plasmons are investigated here in an InGaAs/InP HEMT with a 9 μm period grating gate at 78 and 106 GHz free-space radiation and 4K sample temperature. The dependence of the photoresponse on applied Source-Drain bias is also investigated. The minimum noise equivalent power (NEP) is estimated to be 113 pW/Hz$^{1/2}$, with maximum responsivity of 200 V/W. Such plasmonic alterations in channel conductance provide a means for voltage-tunable THz and sub-THz detectors or filters.

Keywords: HEMT, Plasmon, terahertz, Graphene, 2DEG, detector

1. INTRODUCTION

The THz regime has numerous applications that range from chip-scale optoelectronic spectrometers to airborne multispectral detection and associated IR countermeasures. This frequency range, on the other hand, has been technologically challenged by a dearth of adequate detectors and sources, the so called "THz Gap", despite considerable development effort in recent years. As outlined in [1], plasmonic devices based on 2DEGs in GaAs-based FETs [1-11], GaN HEMTs [12], InGaAs/InP HEMTs [13-19], MOSFETs [20-21], and Graphene [22] are promising THz detector candidates. They combine an ability to confine THz free-space radiation to subwavelength structures (~λ/100) with an ability to bridge between microwave electronics and infrared photonics. In particular, GaAs-based HEMTs have been developed for THz resonant detection [2-7], field enhancement [11], and mixers [9-10]. In these devices, coupling structure geometries have progressed from simple lamellar gratings [2-4] to split gratings [5], nano-antennas, and hybrid antenna-grating structures [1, 6-8].

Technological developments are comparatively less well advanced in the InGaAs/InP materials system [13,14], which nevertheless merits attention due to its potentially ~1-2 orders of magnitude higher sheet charge density and lower electron effective mass. These features would enable functionality at higher THz frequencies than GaAs-based devices. Furthermore, lattice matched growth of InGaAs/InAlAs heterostructures on InP substrates enables integration with other established InP-based photonics and fast electro-optic integrated circuits. In this paper, we present new data on grating-gated InGaAs/InP HEMT plasmonic photoresponse, especially its dependence on Source-Drain bias.

2. THEORY

The dispersion relation for 2D-plasmons for zero Source-Drain bias is given by [23]

$$\omega_n^2 = \frac{e^2 n_s q_n}{m^* \varepsilon_0}\left[\varepsilon_b + \varepsilon_t \coth(q_n d)\right]^{-1}, \quad (1)$$

where ω_n is the frequency of the n[th] integer order plasmon, e the electron charge, m^* is the effective mass (0.043 m_0 for InGaAs), d the 2DEG depth from the grating, n_s the 2DEG sheet charge density, and ε_t (ε_b) the relative permittivity of the semiconductor layers above (beneath) the 2DEG, respectively. The allowed plasmon wavevector, q_n, takes discrete values $2\pi n/a$, and accounts for the momentum mismatch between plasma waves and free-space radiation.

If the top gate is close enough to the 2DEG layer ($q_n d << 1$), the dispersion relation reduces to

$$\omega_n^2 = \frac{e^2 n_s d}{m^* \varepsilon_0 \varepsilon_t} q_n \quad . \tag{2}$$

Eq. 2 is the most well-known 2DEG plasmon dispersion relationship which is relevant the device of this work, with $q_n d \sim 0.02$. In an unbiased device ($V_{SD} \sim 0\ V$) the left and right propagating plasmons are symmetrical and the superposition of the two will result in the formation of 2D-plasmon standing waves. A DC bias V_{SD} applied between source and drain causes electron drift with velocity v_0, breaking the symmetry and drastically changing the plasmonic photoresponse. Then the dispersion for the two different plasmonic modes when $q_n d << 1$ becomes [24]

$$\gamma_{1,2} = \alpha_{1,2} + j\beta_{1,2} = \frac{\left(\frac{v_0}{\tau} + 2jv_0\omega\right) \pm \sqrt{\Delta}}{2\left(v_0^2 - 4Ad\right)}, \tag{3}$$

$$\Delta \equiv \frac{v_0^2}{\tau^2} - 16Ad\omega^2 + 16j\frac{Ad\omega}{\tau}$$

where γ is the complex plasmon wavevector, τ is the relaxation time, $A = n_s e^2/4\varepsilon_t\varepsilon_0 m^*$, and α and β are attenuation and phase constants, respectively. For a resonant, unbiased device ($\omega\tau > 1$ and $v_0 \approx 0\ m/s$) Eq. 3 reduces to Eq. 2 for a grating coupler with the real wavevector of $\beta = q_n = 2\pi n/a$.

Sheet charge density, n_s, is required to calculate the frequencies of different order plasmon modes as well as to calculate the absorption spectrum. The n_s is derived from the applied gate bias and temperature dependence carrier concentration in the absence of the quantum well, n_d, by [13]

$$n_s = \frac{\varepsilon_t \varepsilon_0}{ed}\left(V_g - \phi_b + E_c + \frac{en_d d}{\varepsilon_t \varepsilon_0}\right) \quad , \tag{4}$$

where V_g is the applied gate bias, $\phi_b = 0.7\ eV$ is the Schottky barrier height for the metal/Group III-V contacts, and E_c is the conduction band offset calculated to be 0.675 eV for the device of this work following the method in [13, 25].

3. EXPERIMENTAL DETAILS

The double quantum well (DQW) InGaAs/InP HEMT structure was identical to that in [14, 16-17], and the grating gate had 9 µm period with 22% duty cycle. The layer structure is presented in figure 1.

75 Å n^+-$In_{0.6}Ga_{0.4}As$ 6.0x10^{18} cm^{-3} Cap
350 Å $In_{0.52}Al_{0.48}As$ Undoped
Si δ-doping 4x10^{12} cm-2
30 Å $In_{0.52}Al_{0.48}As$ Undoped Spacer
200 Å $In_{0.68}Ga_{0.32}As$ Channel
30 Å $In_{0.52}Al_{0.48}As$ Undoped Spacer
Si δ-doping 4x10^{12} cm-2
3000 Å $In_{0.52}Al_{0.48}As$ Buffer
InP Substrate

Fig. 1. MBE grown epilayer structure used for fabrication of the HEMT

The n_d and τ values were determined from 4 K Source-Drain I-V curves according to Ref. [13]. Relaxation time τ at 4 K was determined to be 0.18 ps and n_d to be 1.55 × 10^{12} cm^{-2}, respectively. While, the n_d derived here agrees with the previously reported value [14], relaxation time is half what we determined before. This might be attributed to aging of the sample and degradation of the Ohmic contacts of the device.

For I-V and photoresponse measurements, the sample was mounted inside a closed cycle cryostat and maintained at 4 K. Radiation at 78 or 106 GHz was generated by a backward wave oscillator (BWO). The experimental setup was modified from that of Ref [14] to reduce standing wave interferences and polarization scrambling by conducting the beam into cryostat vacuum via a mylar-sealed rectangular waveguide. In this way, the output of the polarization-preserving horn was placed just 7 mm above the sample with no intermediary window.

The amplitude of the radiation power was modulated electronically at 512 Hz. A crystal detector connected via a 10 dB directional coupler monitored the modulated power. The output signal of the crystal detector was high-pass filtered and amplified to serve as the lock-in reference. Constant voltages of 0, 0.25, or 0.5 V were applied to the source while the drain was connected to ground via a 100 Ω load. The gate-bias (V_g) was stepped from -0.5 to 0.8 V with respect to ground in increments of 10 mV. The voltage across the load resistor was input to the lock-in for synchronous amplification of the photoresponse.

4. RESULTS

The low-frequency portions of calculated plasmon-resonance-band spectra (following [26-27]) are presented in figure 2 for $V_{SD} = 0$ V as a function of V_g. At these low frequencies, fundamentals and harmonics have merged and the resonance bands are broad. The peak positions shift from 295 to 550 GHz with increasing V_g due to the increase in n_s, in agreement with Eq. 1. The vertical dashed lines mark the two excitation frequencies of 78 and 106 GHz, which lie within the plasmon resonance absorption bandwidth. These frequencies happen to be in the range where the absorption spectra at different V_g values, experience drastic slope changes.

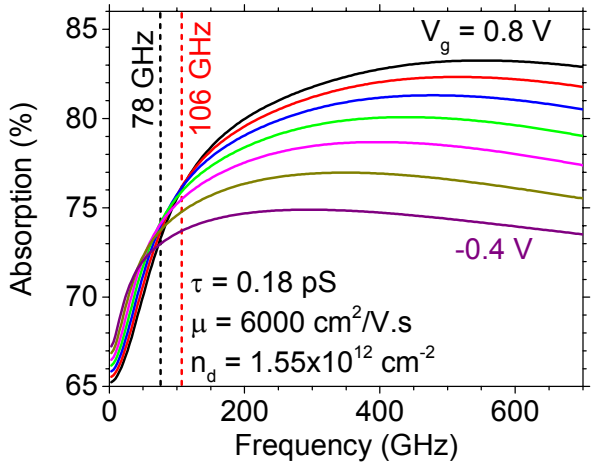

Fig. 2. Calculated absorption spectra of the device at different V_g. Two measurement frequencies are marked by vertical dashed lines.

The measured photoresponse of the unbiased device is presented in figure 3 as a function of V_g for the two excitation frequencies. Data for two different polarizations with E-field perpendicular or parallel to the grating bars are presented. The response for parallel polarization is expected to be zero since such should fail to polarize the grating and produce plasmon-exciting local fields, and indeed the response for parallel polarization at 78 GHz is 6x weaker than for perpendicular polarization. The parallel response can be explained by a misalignment of as little as 5 deg or by scattering off metal parts [14]. We note that the polarization dependence with the new setup is now much stronger that previously reported [14, 16-18]. For comparison, the calculated absorption at 78 and 106 GHz are also plotted as a function of V_g in Fig. 3 on the right vertical axis. The absorption curves peak at V_g values of 0.22 and 0.5 V for 78 and 106 GHz radiation, respectively.

The measured photoresponse agrees qualitatively with the calculations in a number of significant ways. The overall photoresponse to 106 GHz radiation is stronger and broader than the response at 78 GHz, and its maximum occurs at a more positive V_g value. The peak separation for the two frequencies is also about the same for theory and experiment ($\Delta V_g \sim 0.35$ V). The V_g values for the measured peaks are lower than the calculated values by about 0.30-0.35 V. However, a better agreement is found by increasing the value of τ from 0.18 to 0.25 ps in the calculations. This difference is within the likely uncertainty [13] and is smaller than the factor of 2 difference between τ values determined here and previously [14]. Also note that the absorption values vary by only 5% while the photoresponse varies by 88%, suggesting a non-linear response. Such differences between photoresponse and absorption have been observed previously and in other systems, while the plasmonic absorption in group III-V heterostructures are ~ 4-5% at resonance, a resonant photoresponse of 9-times stronger than the baseline is reported for GaAs-devices [2]. Another observation is that the measured photoresponse peaks are sharper than the theoretical ones, which can also result from a non-linearity.

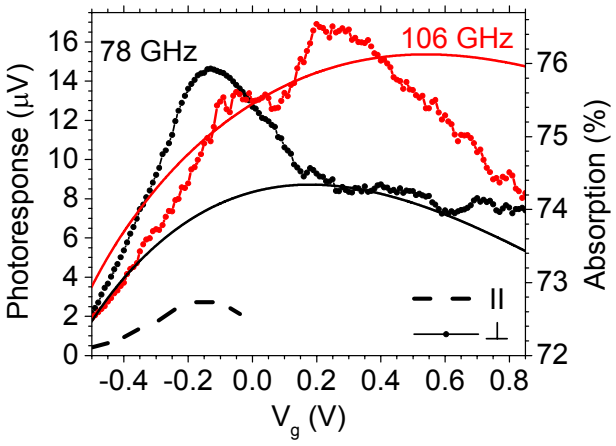

Fig. 3. Calculated absorption of the device along with the measured photoresponse as a function of the applied V_g at free-space frequencies of 78 and 106 GHz. Photoresponse is measured at two different polarizations as indicated by the legend.

Figure 4 presents the measured photoresponse at 78 GHz for different V_{SD} values. The maximum photoresponse decreases almost three-fold when positive V_{SD} is applied. While the unbiased case shows a single peak, indicated by a symbol, two peaks appear with applied V_{SD}. The second peak seems to move toward lower gate biases with increasing V_{SD} . The 1st peak apparently has the opposite V_{SD} dependence. The existence of two peaks for finite V_{SD} is evidence of a change in the plasmonic behavior of the cavity, in qualitative agreement with the existence of two branches in Eq. 3.

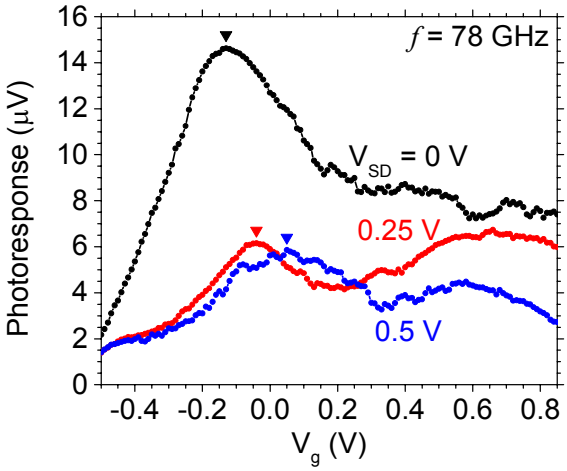

Fig. 4. Measured photoresponse of the InGaAs/InP HEMT to free-space frequencies of 78 GHz at different applied V_{SD} values.

The NEP of the detector is extracted as a function of V_g from the measured photoresponse and is plotted in figure 5 for the two measurement frequencies. In these calculations, $NEP = P/(SNR \times \Delta f^{1/2})$, where P is the radiation power at the device area, $SNR = Photoresponse\ (V_g) / Noise$ and is the signal to noise ratio, and Δf is the measurement bandwidth taken as 0.05 Hz from 10 s lock-in time constant. P is calculated by assuming that the measured 12.2 mW radation power at the input to the horn is uniformly distributed over its 695 mm^2 aperture, giving an intensity of 17.5 μW/mm^2. We assume that diffraction and scattering may reduce the actual intensity ten-fold at the sample. The total power incident on the 195 μm × 250 μm channel is then about 85 nW. The noise was determined to be ~ 5 nV by blocking the radiation and recording the lock-in output.

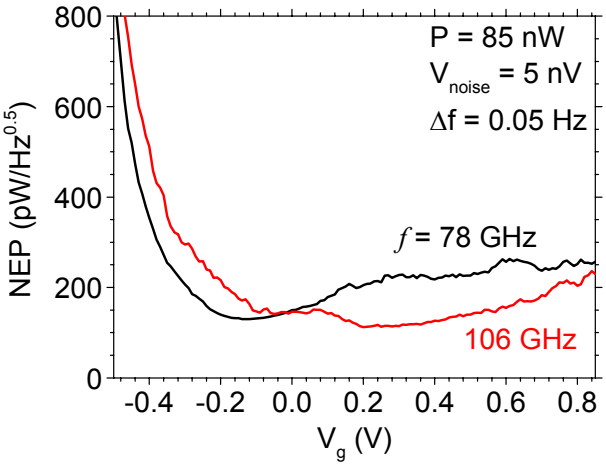

Fig. 5. Calculated NEP of the device for the two measurement frequencies. The minimum measured NEP is 113 pW/Hz$^{1/2}$ at 106 GHz.

From Fig. 5, the minimum NEP value is determined to be 113 pW/Hz$^{1/2}$ and is measured at the peak of the response to the 106 GHz radiation. This is comparable to the previously reported values in [14, 18]. The smaller value reported for InGaAs/InP based detectors at room temperature by [19] at 1 THz radiation can be partly attributed to the higher measurement frequency (higher $\omega\tau$) and more efficient collection with a narrow band antenna. The peak responsivity of our detector is calculated from the estimated incident power at the device and its peak photoresponse to be 200 V/W which is approximately equal to the value reported in [14].

5. SUMMARY

In summary, we presented gate-bias tunable electrical photoresponse to sub-THz radiation in InGaAs/InP HEMTs at two frequencies of 78 and 106 GHz which are well within the plasmon resonance bandwidth. The photoresponse was measured for both unbiased ($V_{SD} \sim 0$ *V*) and biased ($V_{SD} > 0$ *V*) configurations. We attribute the measured photoresponse to excitation of plasmons in the 2DEG and transduction of that absorption to a change in channel conductance, because results agree with theoretical predictions in a number of significant ways. Parameters such as responsivity and NEP were estimated and compared to devices fabricated in the same materials system. Interpretation of the results presented here remains a work in progress. Such a device may find application as a chip-scale tunable sub-THz detector, which can potentially be scaled to higher THz frequencies when a grating-gate coupler with smaller period is used.

6. ACKNOWLEDGMENTS

This work is supported by Air Force Office of Scientific Research. N.N.E and J.W.C acknowledge AFOSR LRIR No. 12RY10COR (Program Officer Dr. Gernot Pomrenke). R.E.P acknowledges grant No. FA95501010030. J.R.H would also like to acknowledge support from AFOSR under LRIR No. 12RY05COR.

REFERENCES

[1] Dyer G. C.,Aizin, G. R., Preu, S., Vinh, N. Q., Allen, S. J., Reno, J. L., and Shaner, E. A., "Inducing an Incipient Terahertz Finite Plasmonic Crystal in Coupled Two Dimensional Plasmonic Cavities." Phys. Rev. Lett., 109, 126803 (2012).

[2] Shaner, E. A., Lee, M., Wanke, M. C., Grine, A. D., Reno, J. L., and Allen, S. J., "Single-quantum-well grating-gated terahertz plasmon detectors," Appl. Phys. Lett, **87**, 193507 (2005)

[3] Peralta, X. G., Allen, S. J., Wanke, M. C., Harff, N. E., Simmon, J. A., et al., "Terahertz photoconductivity and plasmon modes in double-quantum-well field-effect transistors," Appl. Phys. Lett. **81,** 1627-1629 (2002)

[4] Knap, W., Deng, Y., Rumyantsev, S., Shur, M. S., "Resonant detection of subterahertz and terahertz radiation by plasma waves in submicron field-effect transistors," Appl. Phys. Lett. **81**, 4637-4639 (2002)

[5] Shaner, E. A., Grine, A. D., Wanke, M. C., Lee, M., Leno, J. L., and Allen, S. J., "Far-Infrared Spectrum Analysis Using Plasmon Modes in a Quantum-Well Transistor" IEEE Photon. Technol. Lett. **18**, 1925 (2006).
[6] Dyer, G. C., Aizin, G. R., Reno, J. L., Shaner E. A., and Allen, S. J., "Novel Tunable Millimeter-Wave Grating-Gated Palsmonic Detectors", IEEE J. Sel. Top. Quantum Electron. **17**, 85 (2011).
[7] Dyer, G. C., Preu, S., Azin, G. R., Mikalopas, J., et al., "Enhanced performance of sub-terahertz detection in a plasmonic cavity," Appl. Phys. Lett. **100**, 083506 (2012)
[8] Dyer, G. C., Azin, G. R., Allen, S. J., Grine, A. D., Bethke, D., Reno, J. L., and Shaner, E. A., "Induced Transparency by coupling of Tamm and defect states in tunable terahertz plasmonic crystals", Nature Photon. 7, 925 (2013)
[9] Lee, M., Wanke, M. C., and Reno, J. L., "Millimeter-wave mixing using plasmon and bolometric response in a double-quantum-well field-effect transistor," Appl. Phys. Lett., 86, 033501 (2005)
[10] Satou, A., Ryzhii, V., Khmirova, I., Ryzhii, M., and Shur, M. S., "Characteristics of a terahertz photomixer based on a high electron mobility transistor structure with optical input through the ungated regions," J. Appl. Phys. 96, 2084 (2004)
[11] Davoyan, A. R., Popov, V. V., and Nikitov, S. A., "Tailoring Terahertz Near-Field Enhancement via Two-Dimensional Plasmons," Phys. Rev. Lett. 108, 127401 (2012)
[12] Muravjov, A. V., Veksler, D. B., Popov, V. V., Polischuk, O. V., Pala, N., Hu, X., Gaska, R., Saxena, H., Peale, R. E., and Shur, M. S., "Temperature dependence of plasmonic terahertz absorption in grating-gate gallium-nitride transistor structures," Appl. Phys. Lett. 96, 042105 (2010).
[13] Saxena, H., Peale, R. E., and Buchwald, W. R., "Tunable two-dimensional Plasmon resonances in an InGaAs/InP HEMT," J. Appli. Phys. **105,** 113101 (2009).
[14] Nader Esfahani, N., Peale, R. E., Buchwald, W. R., Fredricksen, C. J., Hendrickson, J. R., and Cleary, J. W., "Millimeter-wave photoresponse due to excitation of two-dimentional plasmons in InGaAs/InP high-electron-mobility transistors," J. Appl. Phys., 114, 033105 (2013)
[15] Nader Esfahani, N., Peale, R. E., Fredricksen, C. J., Cleary J. W., Hendrickson, J. R., Buchwald, W. R., Dawson, B. D., Ishigami, M., "Plasmon absorption in grating-coupled InP HEMT and graphene sheet for tunable THz detection," Proc. SPIE 8261, 82610E (2012)
[16] Nader Esfahani, N., Peale, R. E., Buchwald, W. R., Hendrickson, J. R., and Cleary J. W., "Millimeter and terahertz detectors based on plasmon excitation in InGaAs/InP HEMT devices," Proc. SPIE 8624, 86240Q (2013)
[17] Nader Esfahani, N., Peale, R. E., Buchwald, W. R., Hendrickson, J. R., and Cleary J. W., "First observation of a plasmon-mediated tunable photoresponse in a grating-gated InGaAs/InP HEMT for millimeter-wave detection," Proc. SPIE 8512, 85120Y (2012)
[18] El Fatimy, A., Teppe, F., Dyakonova, N., Knap, W., Seliuta, D., Valusis, G., Shchepetov, A., Roelens, Y., Bollaert, S., Cappy, A., and Rumyantsev, S., "Resonant and voltage-tunable detection in InGaAs/InP nanometer transistors," Appl. Phys. Lett. 89, 131926 (2006)
[19] Otsuji, T., Watanabe, T., Boubanga Tombet, S.A., Satou, A., Knap, W. M., Popov, V.V., Ryzhii, M., Ryzhii, V., "Emission and Detection of Terahertz Radiation Using Two-Dimensional Electrons in III-V Semiconductors and Graphene," IEEE Trans. On THz Science and Tech. 3, 63 (2013)
[20] Allen, S. J. Jr., Tsui D. C., and Logan, R. A., "Observation of the Two-Dimensional Plasmon in Silicon Inversion Layers," Phys. Rev. Lett. **38**, 980 (1977).
[21] Tauk, R., Teppe, F., Boubanga, S., Coquillat. D., Knap, W., Meziani. Y. M., Gallon, C., Boeuf, F., Skotnicki, T., Fenouillet-beranger, C., Maude, D. K., Rumyantsev, S., amd Shur, M. S., "Plasma wave detection of terahertz radiation by silicon field effects transistors: Responsivity and noise equivalent power," Appl. Phys. Lett 89, 253511 (2006)
[22] Vicarelli, L., Vitiello, M. S., Coquillat, D., Lombardo, A., Ferrari, A. C., Knap, W., Polini, M., Pellegrini, V., and Tredicucci, A., "Graphene field-effect transistors as room-temperature terahertz detectors," Nature Materials 11, 865 (2012)
[23] Popov, V. V., Polischuk, O. V., and Shur, M. S., "Resonant excitation of plasma oscillations in a partially gated two-dimensional electron layer," J. Appl. Phy., 98, 033510 (2005)
[24] Khorrami, M. A., El-Ghazaly, S., Yu, S., and Naseem, H., "Terahertz plasmon amplification using two-dimensional electron-gas layers," J. Appl. Phys., 111, 094501 (2012)
[25] Huang, J.-H., Chang, T. Y., and Lalevic, B., "Measurement of the conduction-band discontinuity in pseudomorphic $In_x Ga_{1-x} As/In_{0.52}Al_{0.48}As$ heterostructures," Appl. Phys. Lett., 60, 733 (1992)

[26] Zheng, L., Schaich, W. L., and MacDonald, A. H., "Theory of two-dimensional grating couplers," Phys. Rev. B **41**, 8493 (1990).
[27] Nader Esfahani, N., Peale, R. E., Cleary, J. W., Buchwald, W. R., "Plasmon resonance response to millimeter-waves of grating-gated InGaAs/InP HEMT," Proc. SPIE 8023, 80230R (2011)